

Supplementary Information for:

Kidney cytosine methylation changes improve renal function decline estimation in patients with diabetic kidney disease

Caroline Gluck^{1,2}, Chengxiang Qiu^{*1}, Sang Youb Han^{*3}, Matthew Palmer⁴, Jihwan Park¹, Yi-An Ko^{1,5}, Yuting Guan¹, Xin Sheng¹, Robert L Hanson⁶, Jing Huang⁷, Yong Chen⁷, Ae Seo Deok Park¹, Maria Concepcion Izquierdo¹, Ioannis Mantzaris⁸, Amit Verma⁸, James Pullman⁹, Hongzhe Li⁷, Katalin Susztak^{1,5}

*Contributed equally

1. Department of Medicine, Renal Electrolyte and Hypertension Division, University of Pennsylvania, Philadelphia, PA, USA.
2. Department of Pediatrics, Division of Nephrology, The Children's Hospital of Philadelphia, Perelman School of Medicine, University of Pennsylvania, Philadelphia, PA, USA.
3. Division of Nephrology, Department of Internal Medicine, Inje University College of Medicine, Goyang, Korea.
4. Department of Pathology and Laboratory Medicine, Perelman School of Medicine, University of Pennsylvania, Philadelphia, USA.
5. Department of Genetics, University of Pennsylvania, Philadelphia, PA, USA.
6. Diabetes Epidemiology and Clinical Research Section, National Institute of Diabetes and Digestive and Kidney Diseases, Phoenix, AZ, USA.
7. Department of Biostatistics and Epidemiology, Center for Clinical Epidemiology and Biostatistics, School of Medicine, University of Pennsylvania Perelman, Philadelphia, PA, USA.
8. Department of Medicine, Albert Einstein College of Medicine, Bronx, NY, USA.
9. Department of Pathology Montefiore Medical Center, Bronx, NY, USA

Correspondence:

Katalin Susztak MD, PhD
Perelman School of Medicine, University of Pennsylvania
12-123 Smilow Center for Translational Research
3400 Civic Center Blvd
Philadelphia, PA 19104
215 898 2009
ksusztak@pennmedicine.upenn.edu

Supplementary Information

Supplementary Figure 1. Principal Component Analysis for the primary cohort (n=91)

Supplementary Figure 2. Association between cytosine methylation changes and baseline estimated GFR

Supplementary Figure 3. Principal Component Analysis for the replication kidney cohort (n=85)

Supplementary Figure 4. Ingenuity Pathway Analysis (IPA) for top probes associated with interstitial fibrosis

Supplementary Figure 5. Functional enrichment of 65 replicated probes associated with interstitial fibrosis in tissue specific enhancer regions

Supplementary Figure 6. For top probe, cg20597486, we completed experiments to validate the methylation changes as measured by the Illumina Infinium 450K arrays

Supplementary Figure 7. Correlation of top replicated probe methylation levels with interstitial fibrosis and Cis-gene expression levels

Supplementary Figure 8. Distribution of (a) unadjusted eGFR slope and (b) adjusted eGFR

Supplementary Figure 9. Association between eGFR slope and baseline eGFR and interstitial fibrosis

Supplementary Figure 10. Ingenuity Pathway Analysis (IPA) for top probes associated with CKD progression

Supplementary Figure 11. Correlation of top probes that improve CKD progression model methylation levels with Cis-gene expression levels

Supplementary Figure 12. Principal Component Analysis for the replication blood cohort (n=115)

Supplementary Table 1. Clinical variables associated with degree of interstitial fibrosis

Supplementary Table 2. Demographic and clinical characteristics of replication data cohorts

Supplementary Table 3. Histological characteristics of replication cohort

Supplementary Table 4. Gene Ontology for top methylation probes associated with degree of interstitial fibrosis

Supplementary Table 5. Demographic and clinical characteristics of sub-cohorts

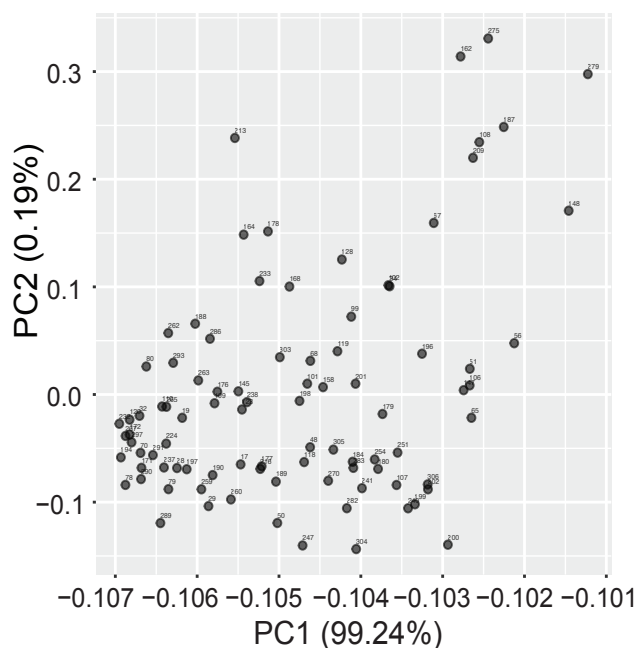
Supplementary Table 6. Longitudinal follow up data by chronic kidney disease (CKD) stage

Supplementary Table 7. Variables associated with eGFR slope

Supplementary Table 8. Progression model with replicated fibrosis-associated probes

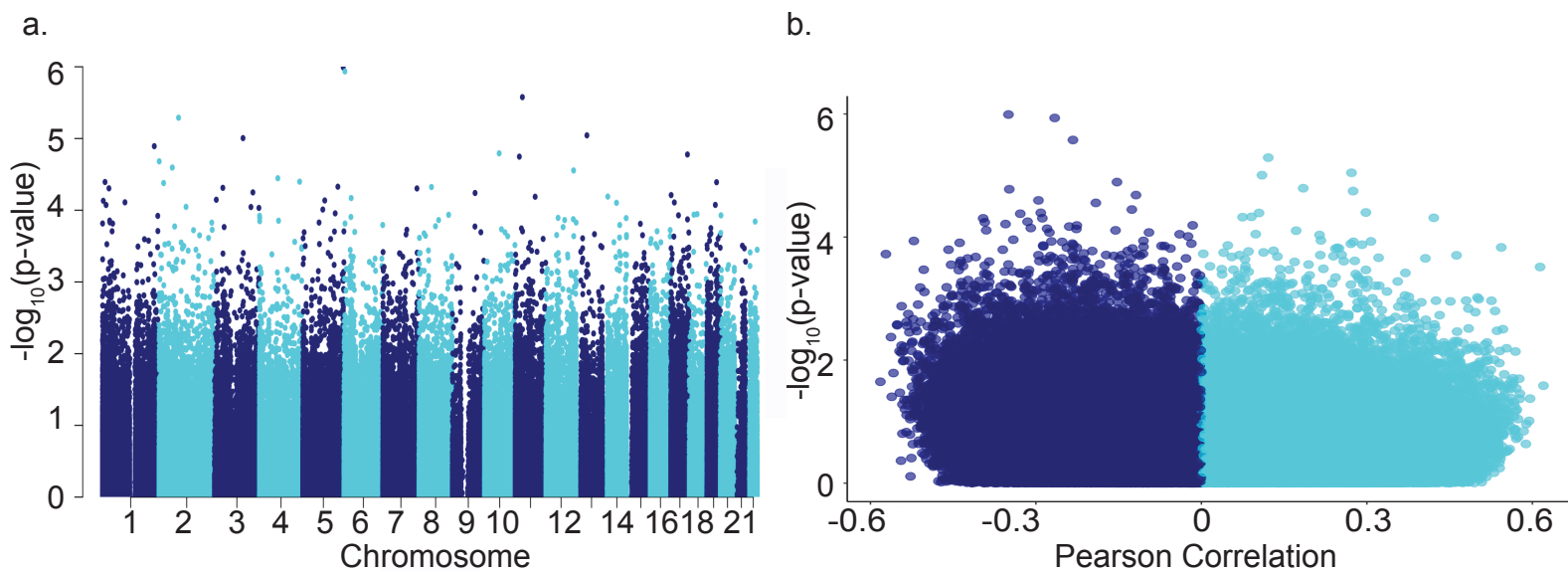
Supplementary Table 9. Gene Ontology for top methylation probes that improve model of kidney function decline

Supplementary Figure 1.



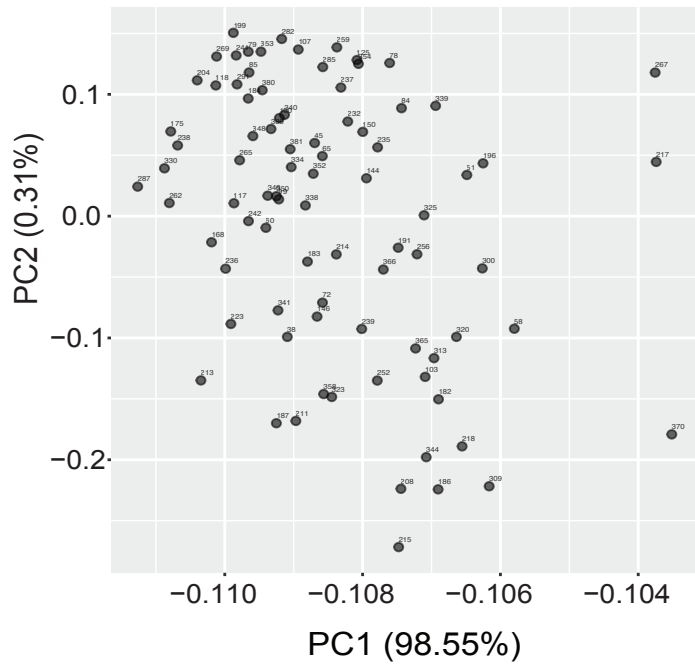
Supplementary Figure 1. Principal Component Analysis for the primary cohort (n=91).

Supplementary Figure 2.



Supplementary Figure 2. Association between cytosine methylation changes and baseline estimated GFR
a. Manhattan plot of eGFR associated methylation changes. The x-axis represents the genomic location of the probe, while the y-axis is the negative base 10 log of the p-value. (The association between the methylation level of 321,473 probes and eGFR was studied using a linear regression models adjusted for age, gender, race, diabetes, hypertension, batch, bisulfite conversion, and lymphocytic infiltrate).
b. Volcano plot depicting the association between eGFR and methylation changes. The x-axis represents the Pearson correlation coefficient of each probe with eGFR. The y-axis is the negative base 10 log of the p-value each probe associated with eGFR.

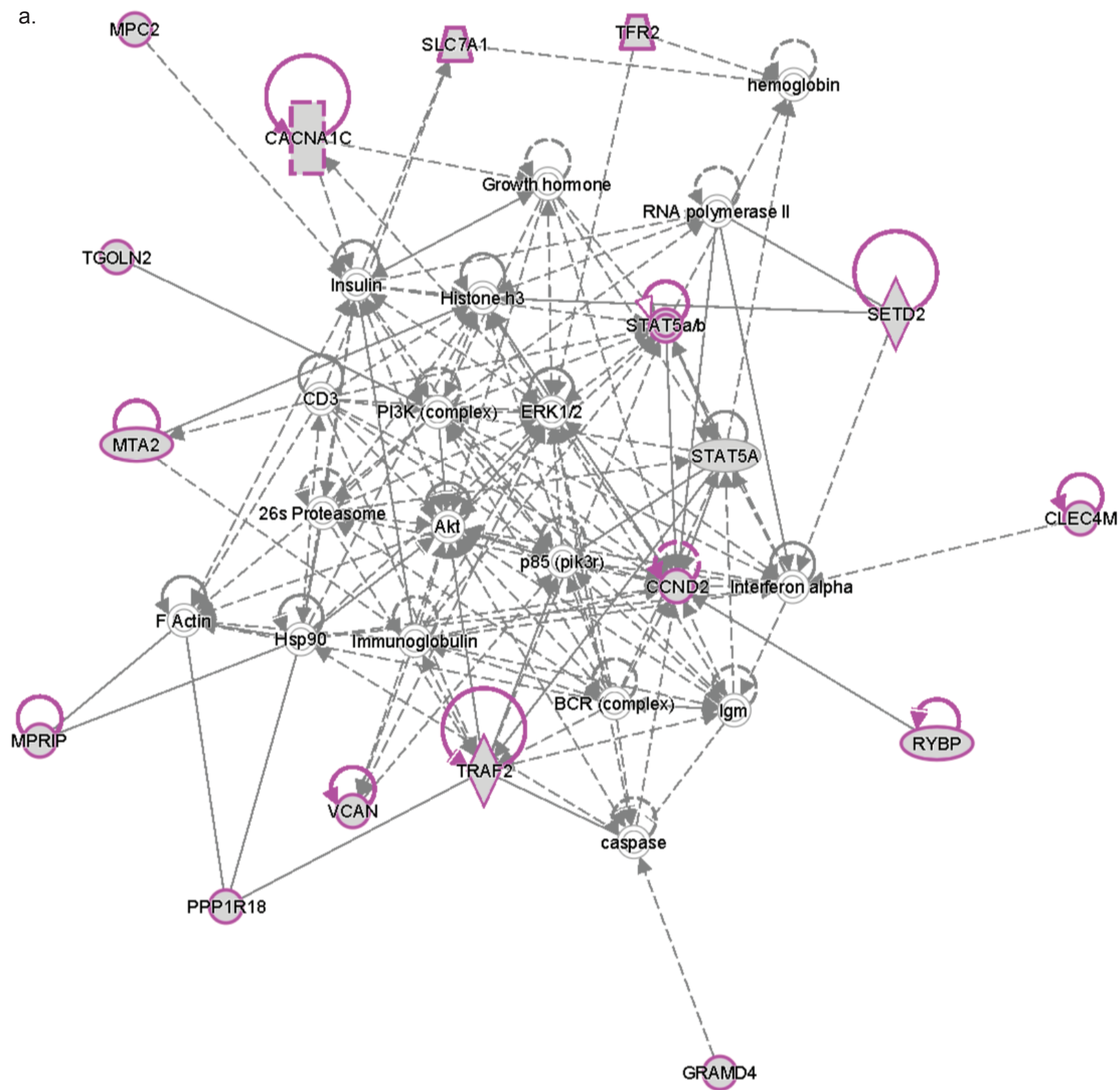
Supplementary Figure 3.



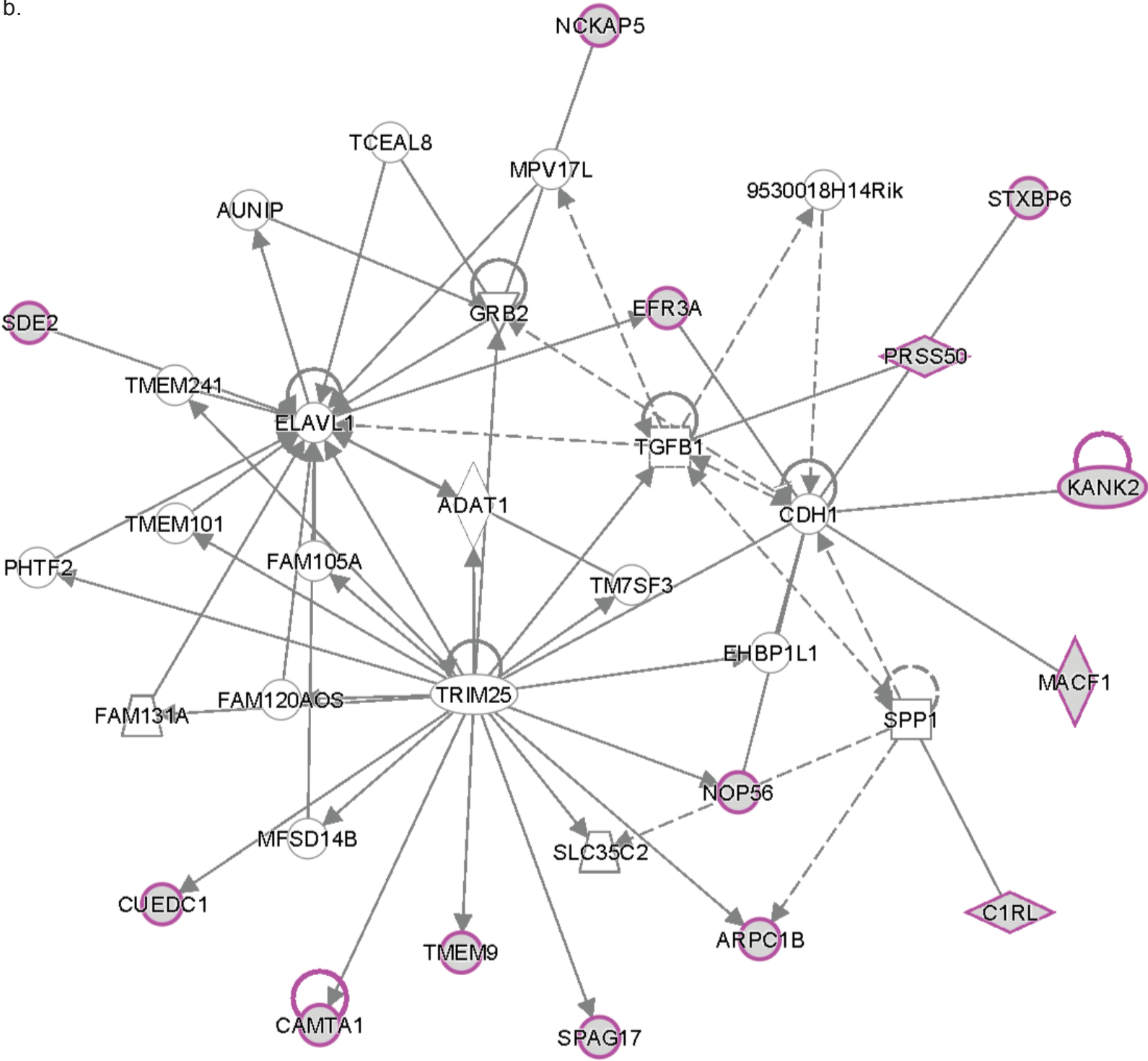
Supplementary Figure 3. Principal Component Analysis for the replication kidney cohort (n=85).

Supplementary Figure 4.

a.

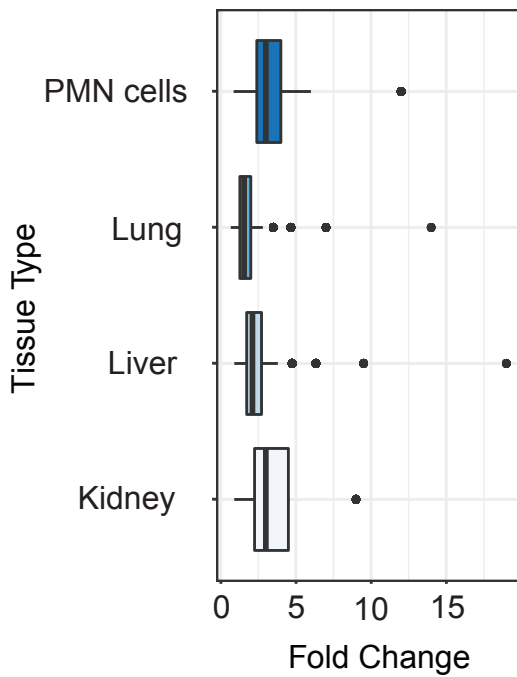


b.



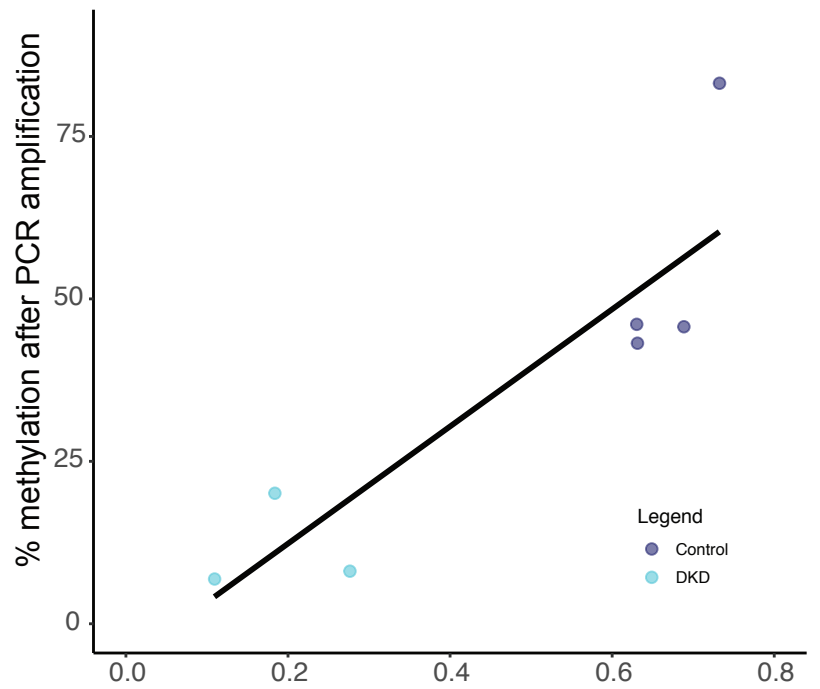
Supplementary Figure 4. Ingenuity Pathway Analysis (IPA) for top probes associated with interstitial Fibrosis. Using proximity matching we identified list of genes differentially methylated which are highlighted
a) Network associated with Cell Death and Survival, Increased Levels of Red Blood Cells, Connective Tissue Development and Function. Score 36.
b) Network associated with Cellular Development, Cellular Movement, Reproductive System Development and Function. Score 31.

Supplementary Figure 5.



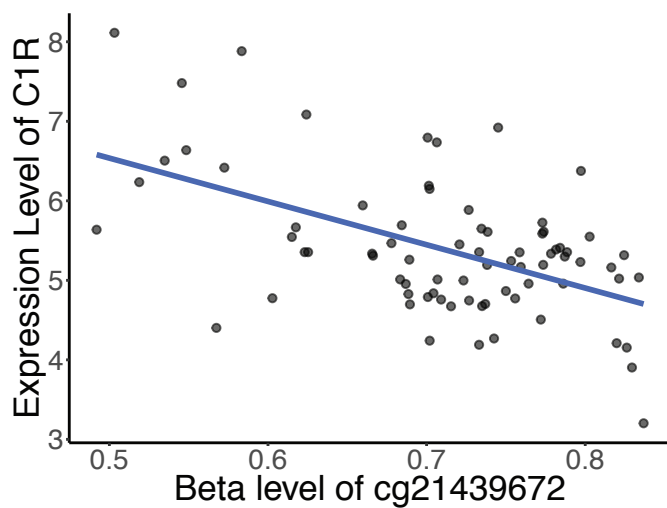
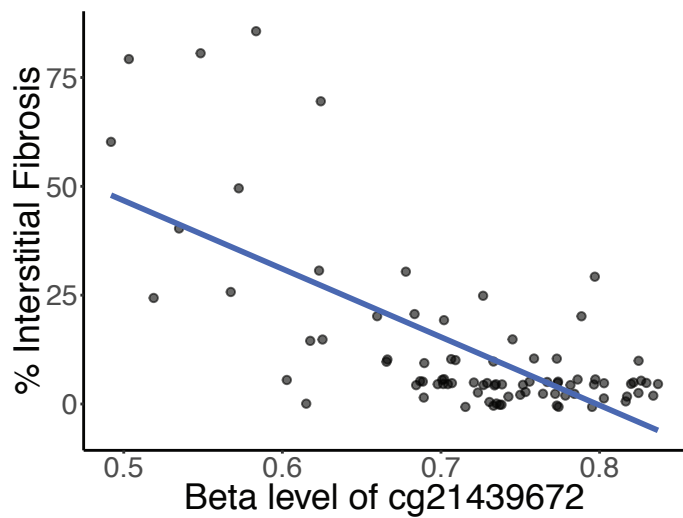
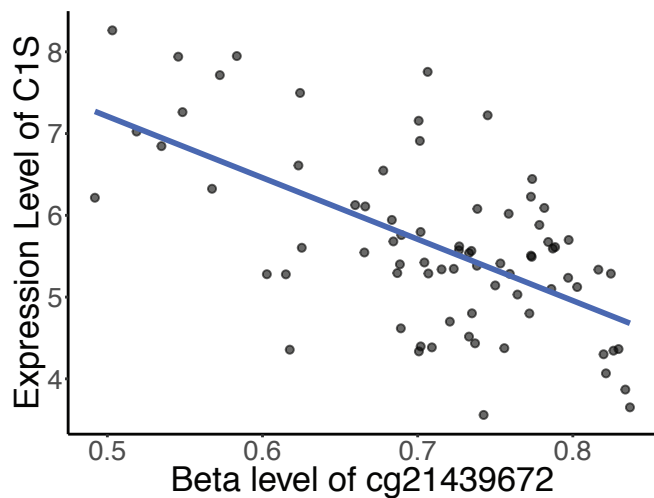
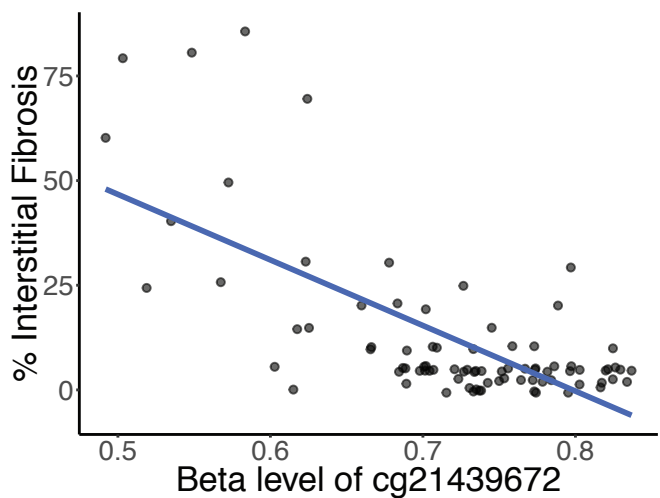
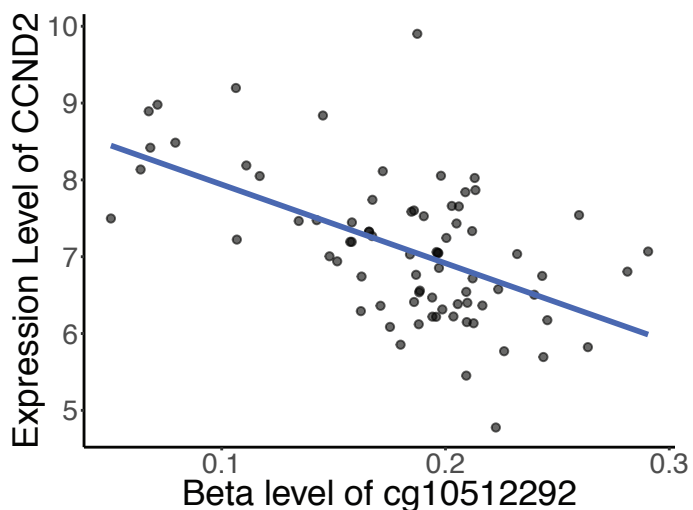
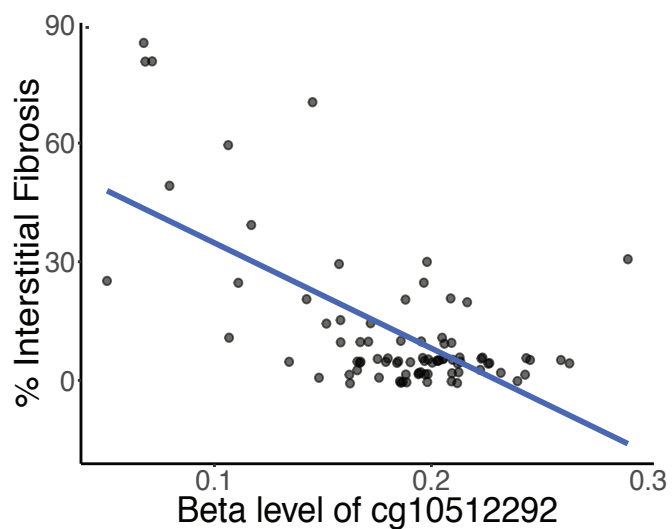
Supplementary Figure 5. Functional enrichment of 65 replicated probes associated with interstitial fibrosis in tissue specific enhancer regions. Fold change compared observed number of significant probes located in each tissue specific enhancer region to the distribution of random 65 probes selected 10,000 times from the background of all array probes used in the regression analysis (n=321,473). Median fold change for kidney enhancer was 4.5. Median fold change for liver enhancer was 2.1. Median fold change for lung was 1.6. Median fold change for polymorphonuclear (PMN) cells was 3.0. (Center line, median fold change; box limits, upper and lower quartiles; whiskers, 1.5x interquartile range).

Supplementary Figure 6.

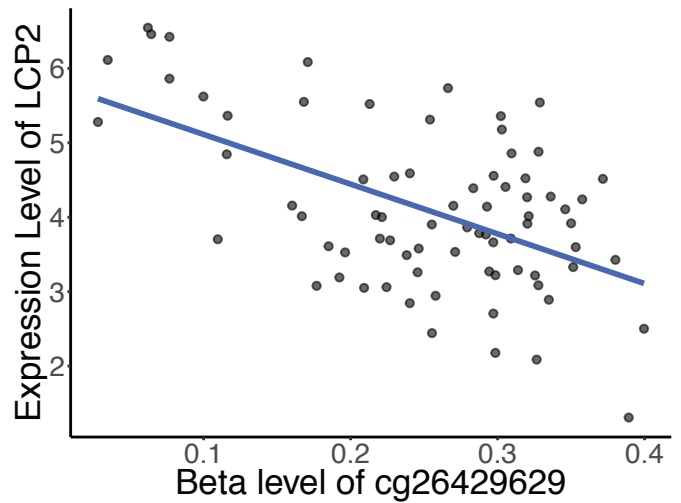
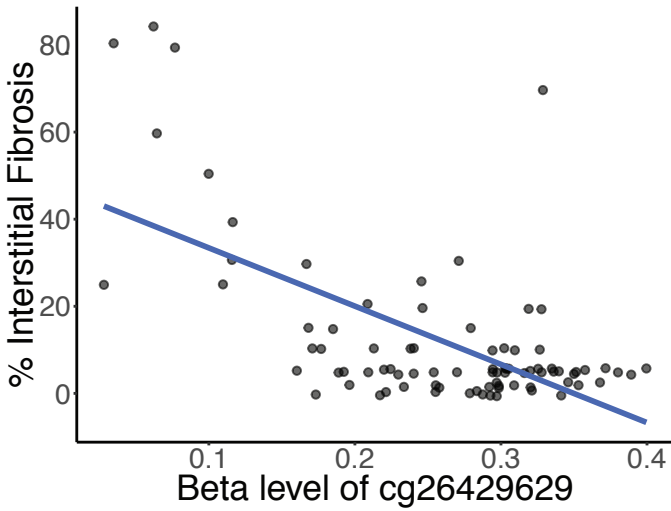
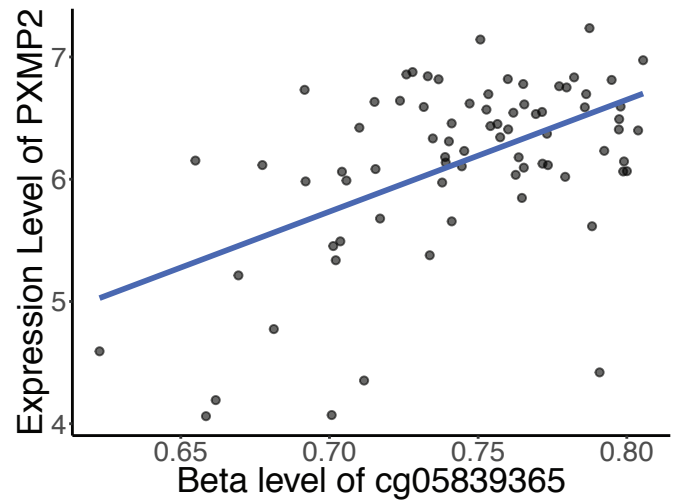
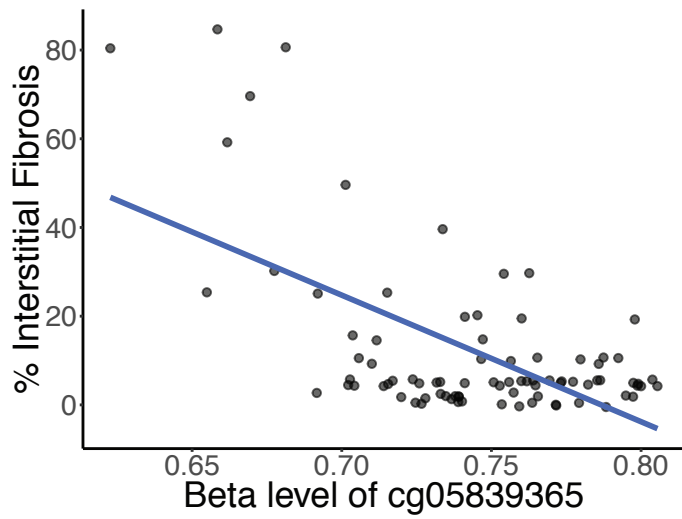


Supplementary Figure 6. For top probe, cg20597486, we completed experiments to validate the methylation changes as measured by the Illumina Infinium 450K arrays. For 3 samples with diabetic kidney disease (DKD) and 4 control samples, we microdissected the human kidney samples and isolated the tubule compartment DNA. DNA was bisulfite converted, amplified with PCR, and transformed into bacteria. 15 colonies were selected per sample and the PCR segment was sequenced. Bisulfite converted sequences were compared with genomic DNA sequence using QUMA: quantification tool for methylation analysis. Pearson correlation coefficient between Illumina Infinium 450k array beta value and percent measure methylation for this loci was 0.88 (p-value = 0.0083).

Supplementary Figure 7.

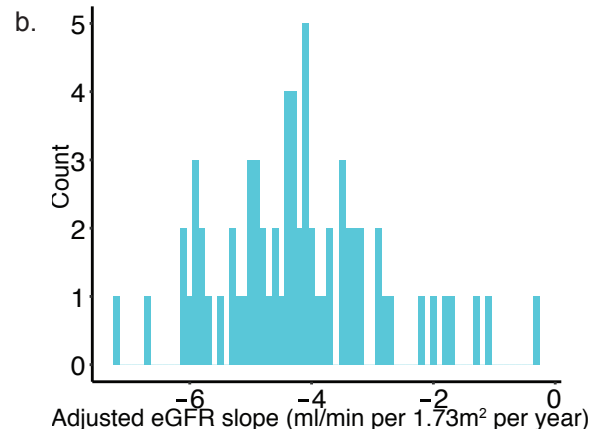
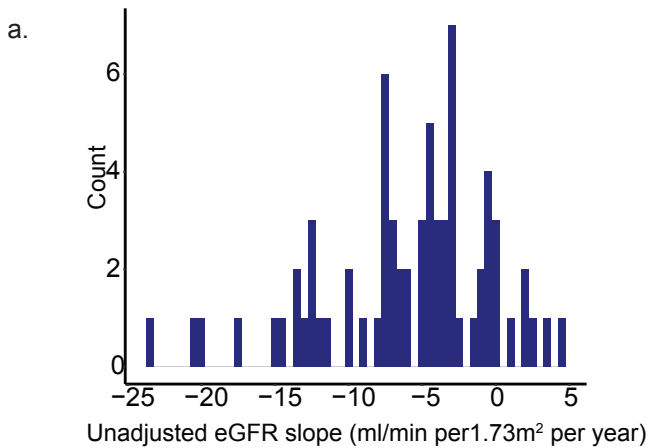


Supplementary Figure 7 continued.



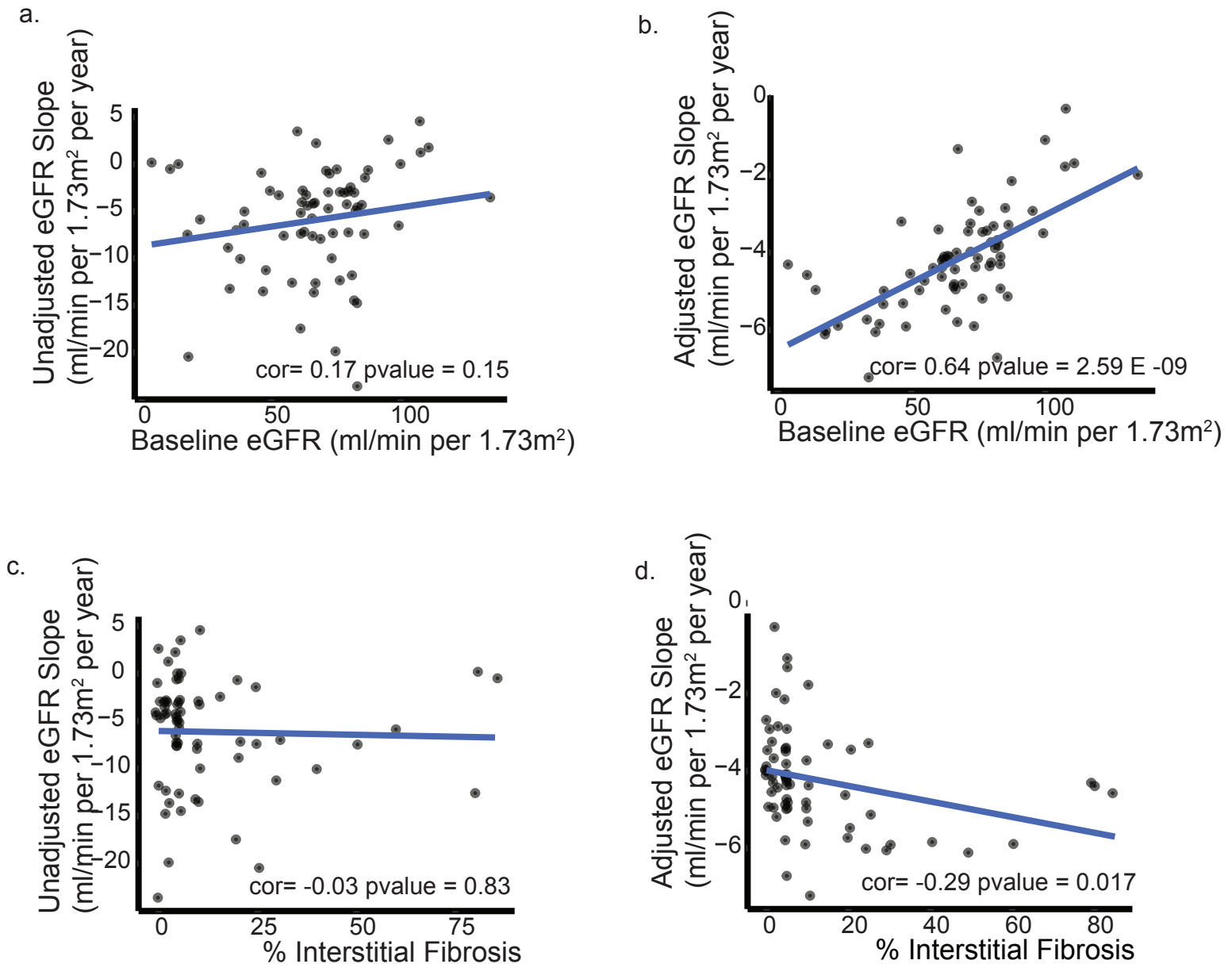
Supplementary Figure 7. Correlation of top replicated probe methylation levels with interstitial fibrosis and Cis-gene expression levels.

Supplementary Figure 8.



Supplementary Figure 8. Distribution of (a) unadjusted eGFR slope and (b) adjusted eGFR

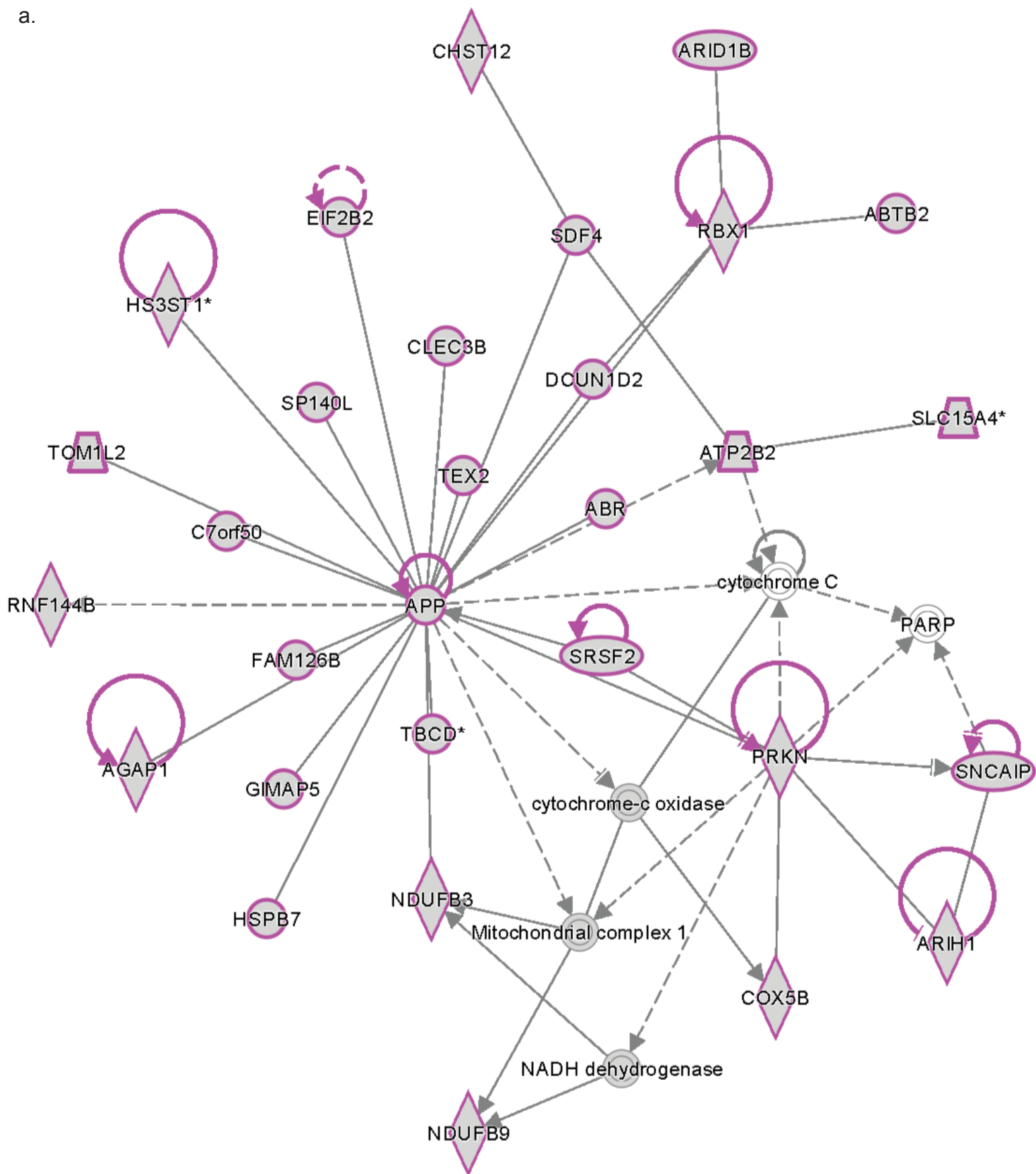
Supplementary Figure 9.



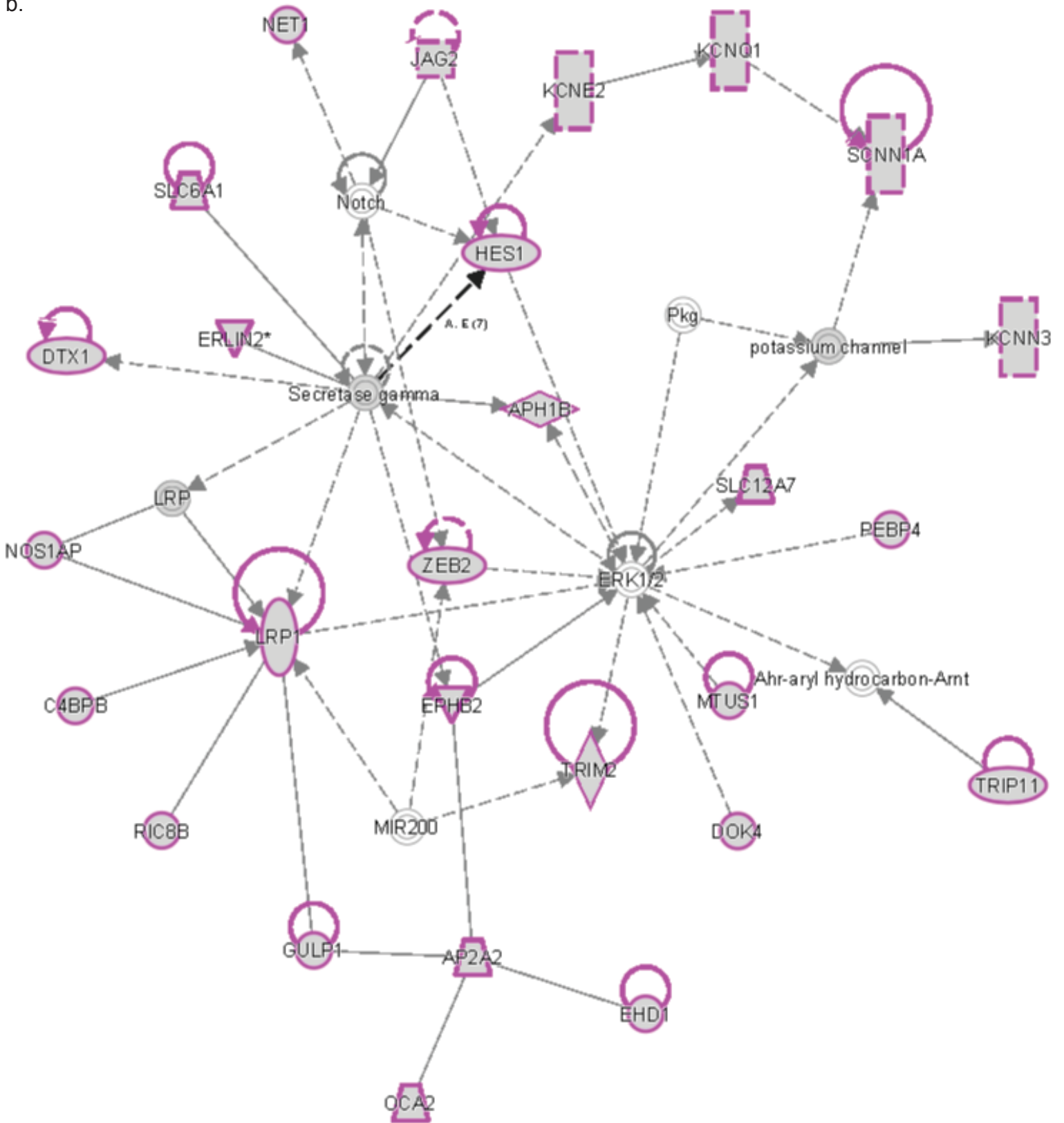
Supplementary Figure 9. Association between eGFR slope and baseline eGFR and interstitial fibrosis. a. Unadjusted eGFR slope is not significantly associated with baseline eGFR in the primary data set using Pearson correlation test. Unadjusted correlation = 0.17 (pvalue = 0.15). b. Adjusted eGFR slope is significantly associated with baseline eGFR in the primary data set using Pearson correlation test. Unadjusted correlation = 0.64 (pvalue = 2.59 e-09). c. Unadjusted eGFR slope is not significantly associated with percent interstitial fibrosis in the primary data set using Pearson correlation test. Unadjusted correlation = -0.03 (pvalue = 0.83). d. Adjusted eGFR slope is significantly associated with percent interstitial fibrosis in the primary data set using Pearson correlation test. Unadjusted correlation = -0.29 (pvalue = 0.017).

Supplementary Figure 10.

a.



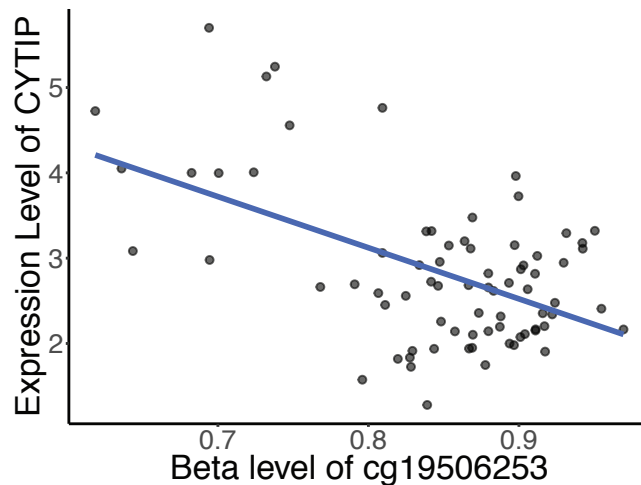
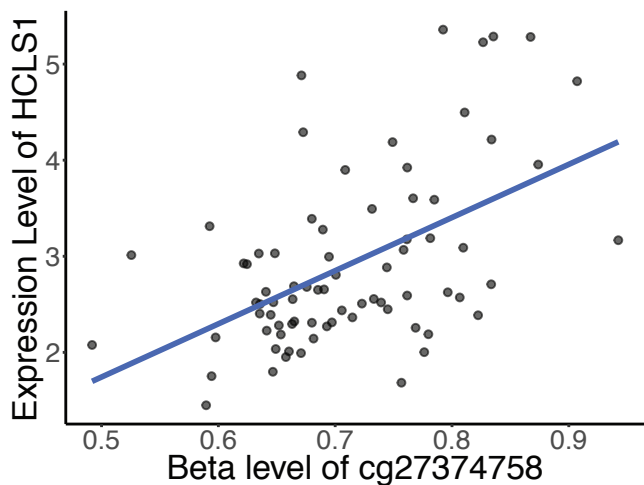
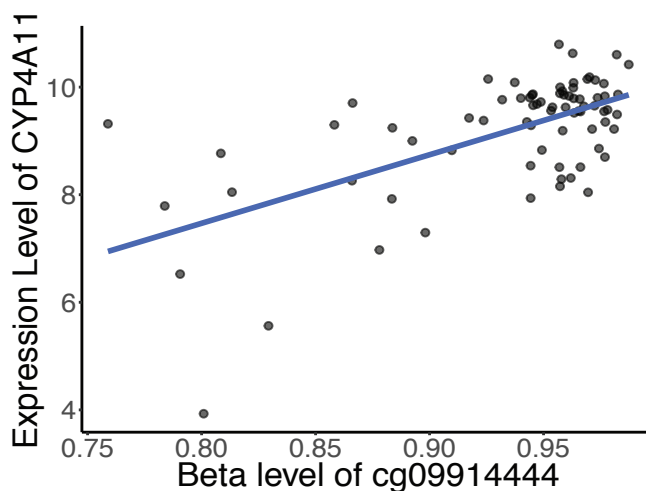
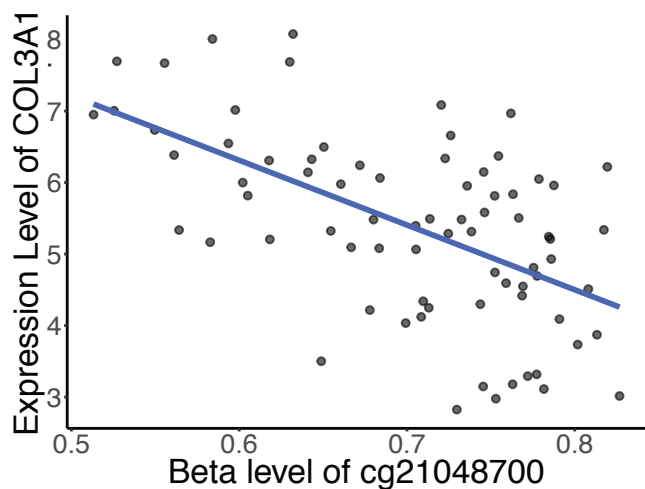
b.



Supplementary Figure 10. Ingenuity Pathway Analysis (IPA) for top probes associated with CKD progression. Using proximity matching we identified list of genes differentially methylated which are highlighted

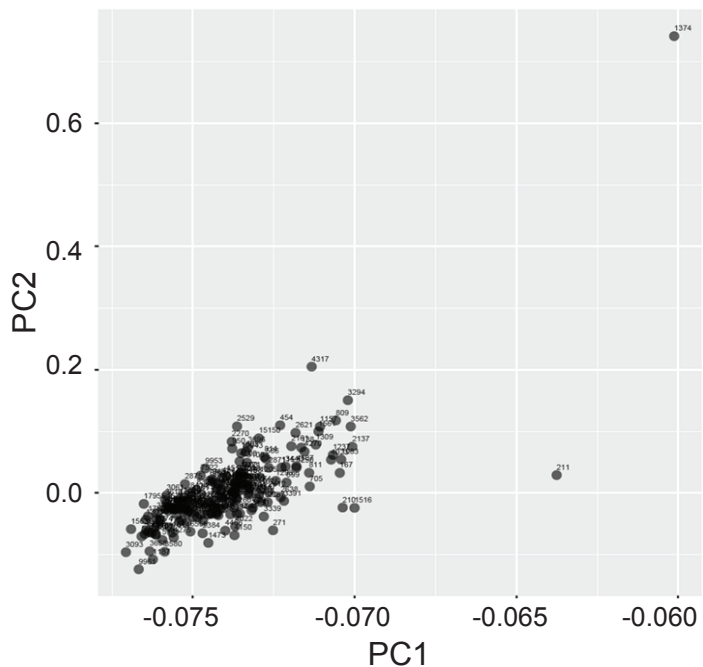
- a) Network associated with Cell-To-Cell Signaling and Interaction, Small Molecule Biochemistry, Neurological Disease. Score 54.
- b) Network associated with Auditory Disease, Auditory and Vestibular System Development and Function, Cell Morphology. Score 46.

Supplementary Figure 11.



Supplementary Figure 11. Correlation of top probes that improve CKD progression model methylation levels with Cis-gene expression levels.

Supplementary Figure 12.



Supplementary Figure 12. Principal Component Analysis for the replication blood cohort (n=115).

Supplementary Table 1. Clinical variables associated with degree of interstitial fibrosis

| Variable | Correlation Coefficient* | P-value* |
|------------------------------|--------------------------|----------|
| Baseline eGFR | -0.6370148 | 7.31E-11 |
| Diabetes | 0.463479 | 9.00E-06 |
| Hypertension | 0.2787701 | 0.01071 |
| Mean Arterial Pressure (MAP) | 0.07641616 | 0.5295 |
| Systolic BP | 0.1475063 | 0.2196 |
| Urine Dipstick (Albuminuria) | 0.5419931 | 1.74E-07 |
| Age | 0.006002272 | 0.9568 |
| Weight | -0.03595815 | 0.75 |
| Height | -0.2027584 | 0.06947 |
| Body Mass Index | 0.04058141 | 0.7225 |
| Sex | -0.03815405 | 0.7304 |
| Race | 0.01945298 | 0.8606 |

* Univariate analysis utilizing two sided Pearson correlation

Supplementary Table 2. Demographic and clinical characteristics of replication data cohorts

| | Replication Cohort (kidney) | Replication Cohort (blood) |
|--|--------------------------------|-------------------------------|
| Subjects (n) | N=85 | N= 115 |
| Baseline eGFR (ml/min per 1.73m ²) | 56.8 (36.4) | 85.4 (27.2) |
| Female | 38 (45%) | 74 (64%) |
| Age | 59.4 (18.0) | 52.3 (11.6) |
| Race | | |
| Asian | 2 (2%) | |
| Caucasian | 6 (7%) | |
| African American | 62 (72%) | |
| Hispanic | 2 (2%) | |
| Multiracial | 9 (11%) | |
| Unknown | 4 (5%) | |
| American Indian | NA | 115 (100%) |
| Diabetes | 21 (25%) | 115 (100%) |
| duration (years) | NA | 17.5 (6.6) |
| Hemoglobin A1C (for DM) | 7.0 (1.7) | 10.1 (2.1) |
| Hypertension | 68 (80%) | NA |
| mean blood pressure (mmHg) | 101.6 (14.6) | 99.3 (10.9) |
| Proteinuria: dipstick (0-5) | 1.5 (1.6) | NA |
| Albumin-creatinine ratio (mg/g) | NA | 1802.7 (2298.0) |
| BMI (kg/m ²) | 28.4 (7.8) | NA |
| End Stage Renal Disease | NA | N=45 |
| Subjects with longitudinal eGFR data (n) | N= 0 | N= 115 |
| Time span (years) | | 5.6 (3.5) |
| Unadjusted GFR Slope (ml/min per 1.73m ² per year) | | -6.5 (6.5) |
| Adjusted GFR Slope (ml/min per 1.73m ² per year) | | -5.8 (3.3) |



Data are mean (SD) or n (%)

Supplementary Table 3. Histological characteristics of replication cohort

| | Replication Cohort |
|-------------------------------------|--------------------|
| n | 75 |
| Hypoperfused Glomeruli (0-3) | 0.77 (0.88) |
| Glomerular Wall Thickening (0-3) | 0.30 (0.68) |
| Mesangial Matrix (0-3) | 0.45 (0.77) |
| Mesangial Cellularity (0-3) | 0.25 (0.60) |
| KW Nodule (0-1) | 0.01 (0.11) |
| Pericapsular Fibrosis (0-2) | 0.94 (0.84) |
| Globally Sclerotic Glomeruli (%) | 25.31 (30.88) |
| Segmentally Sclerotic Glomeruli (%) | 1.16 (3.46) |
| Tubular Atrophy (%) | 28.89 (35.50) |
| Acute Tubular Injury (%) | 3.57 (12.52) |
| Tubules Reabsorption (0-3) | 0.18 (0.46) |
| Interstitial Fibrosis (%) | 27.62 (32.40) |
| Plasmacytic Infiltrate (0-3) | 0.54 (0.69) |
| Lymphocytic Infiltrate (0-3) | 1.24 (0.82) |
| Eosinophilic Infiltrate (0-3) | 0.22 (0.48) |
| Vessel Medial Thickening (0-3) | 0.22 (0.60) |
| Vessel Intimal Fibrosis (0-3) | 1.78 (1.01) |
| Vessel Arteriolar Hyalinosis (0-3) | 0.52 (0.74) |

Data are mean (SD)

Supplementary Table 4. Gene Ontology for top methylation probes associated with degree of interstitial fibrosis

| Category | Term | RT | Genes | Count | % | P-Value | Benjamini |
|-------------|---------------------|----|---|-------|------|----------|-----------|
| GOTERM_BP_1 | Biological adhesion | RT |  | 11 | 22.4 | 5.60E-03 | 1.10E-01 |
| GOTERM_BP_1 | localization | RT |  | 23 | 46.9 | 7.40E-03 | 7.10E-02 |

!

Supplementary Table 5. Demographic and clinical characteristics of sub-cohorts

| | Primary and Replication Cohort (kidney) with Gene Expression Data | Primary Cohort (kidney) with longitudinal eGFR Data |
|---|--|--|
| Subjects (n) | N=77 | N=69 |
| Baseline eGFR (ml/min per 1.73m ²) | 67.5 (26.4) | 66.3 (24.7) |
| Female | 34 (44%) | 38 (55%) |
| Age | 64.9 (11.1) | 64.7 (11.5) |
| Race | | |
| Asian | 3 (4%) | 1 (1%) |
| Caucasian | 17 (22%) | 13 (19%) |
| African American | 24 (31%) | 26 (38%) |
| Hispanic | 5 (6%) | 6 (9%) |
| Multiracial | 14 (18%) | 13 (19%) |
| Unknown | 14 (18%) | 10 (15%) |
| Diabetes | 37 (48%) | 31 (45%) |
| Hypertension | 55 (71%) | 52 (75%) |
| MAP | 94.5 (11.6) | 93.4 (11.7) |
| Proteinuria: dipstick (0-5) | 1 (1.5) | 0.9 (1.4) |
| BMI (kg/m ²) | 31.0 (9.6) | 30.7 (10.0) |

Data are mean (SD) or n (%)

Supplementary Table 6. Longitudinal follow up data by chronic kidney disease (CKD) stage

| CKD stage | GFR (ml/min per 1.73m ²) | Age (years) | % Interstitial Fibrosis | Unadjusted GFR slope (ml/min per 1.73m ² per year) | Adjusted GFR slope (ml/min per 1.73m ² per year) | n |
|-----------|---|-------------|-------------------------|--|--|----|
| 0 | 115.1 (13.1) | 55.3 (6.2) | 4.67 (4.62) | 1.0 (3.4) | -1.4 (0.8) | 4 |
| 1 | 98.2 (2.5) | 56.0 (8.9) | 3.3 (2.9) | -1.3 (4.7) | -2.5 (1.3) | 3 |
| 2 | 73.3 (8.4) | 65.1 (11.7) | 6.3 (6.6) | -6.4 (5.7) | -4.1 (1.0) | 43 |
| 3 | 44.4 (8.2) | 71.0 (9.0) | 22.0 (22.9) | -7.9 (4.1) | -5.3 (1.0) | 13 |
| 4 | 19.4 (2.7) | 64.0 (14.9) | 45.0 (18.0) | -11.3 (8.0) | -6.0 (0.1) | 3 |
| 5 | 9.7 (5.3) | 54.0 (8.0) | 56.6 (44.8) | -0.1 (0.4) | -4.6 (0.3) | 3 |

Data are mean (SD)

Supplementary Table 7. Variables associated with eGFR slope

| Variable | Correlation Coefficient* | P-value* |
|-------------------------------------|--------------------------|----------|
| Baseline eGFR | 0.6428609 | 2.59E-09 |
| Diabetes | -0.5713708 | 2.94E-07 |
| Hypertension | -0.2871806 | 0.01673 |
| Mean Arterial Pressure (MAP) | 0.129615 | 0.3194 |
| Systolic BP | -0.07372888 | 0.5723 |
| Urine Dipstick (Albuminuria) | -0.3493811 | 0.003497 |
| Age | -0.3703063 | 0.001737 |
| Weight | -0.004508233 | 0.9711 |
| Height | 0.2931494 | 0.01606 |
| Body Mass Index | -0.1022956 | 0.4212 |
| Sex | -0.02069567 | 0.866 |
| Race | -0.09740657 | 0.4259 |
| Hypoperfused Glomeruli (0-3) | -0.2170649 | 0.08 |
| Glomerular Wall Thickening (0-3) | -0.1270326 | 0.3094 |
| Mesangial Matrix (0-3) | -0.3223249 | 0.008831 |
| Mesangial Cellularity (0-3) | -0.2293743 | 0.06394 |
| KW Nodule (0-1) | -0.1182092 | 0.3445 |
| Pericapsular Fibrosis (0-2) | -0.3310049 | 0.006634 |
| Globally Sclerotic Glomeruli (%) | -0.1320976 | 0.3144 |
| Segmentally Sclerotic Glomeruli (%) | -0.01834522 | 0.8838 |
| Tubular Atrophy (%) | -0.280921 | 0.02232 |
| Acute Tubular Injury (%) | -0.2301258 | 0.06516 |
| Tubules Reabsorption (0-3) | -0.2140474 | 0.08944 |
| Interstitial Fibrosis (%) | -0.2928217 | 0.01703 |
| Plasmacytic Infiltrate (0-3) | -0.1514714 | 0.2284 |
| Lymphocytic Infiltrate (0-3) | -0.3039231 | 0.01384 |
| Eosinophilic Infiltrate (0-3) | -0.2120453 | 0.08994 |
| Vessel Medial Thickening (0-3) | -0.07113111 | 0.5765 |
| Vessel Intimal Fibrosis (0-3) | -0.01431152 | 0.9106 |
| Vessel Arteriolar Hyalinosis (0-3) | -0.1099817 | 0.3794 |

* Univariate analysis utilizing two sided Pearson correlation

Supplementary Table 8. Progression model with replicated fibrosis-associated probes

| Variable ^a | Model ^b | | | % Explained by Variable ^c | | |
|------------------------------------|--------------------|-----------------------------------|-----------------------------------|--------------------------------------|------------|------------|
| | Base | Base + Probe cg00355019 (A) | Base + Probe cg07830160 (B) | Base Model | Model A | Model B |
| Baseline GFR | 0.03*** | 0.04*** | 0.04*** | 20.67 | 31.41 | 30.17 |
| Diabetes | - 0.72* | - 1.11*** | - 1.05*** | 5.75 | 9.51 | 8.40 |
| Age | - 0.03 | - 0.01 | - 0.01 | 6.16 | 0.85 | 0.69 |
| CpG probe | NA | - 1.17*** | -1.55*** | NA | 13.19 | 11.89 |
| Methylation Batch | NA | NA | NA | NA | 8.49 | 13.02 |
| Bisulfite conversion | NA | 0.42 | 1.96 | NA | 0.00 | 0.03 |
| R2 | 0.51 | 0.70 | 0.70 | | | |
| Adjusted R2 | 0.49 | 0.64 | 0.63 | | | |
| Akaike Information Criterion | 206.1 | 189.6 | 191.1 | | | |
| P-value | 3.13e-10 | 6.33e-11 | 1.10e-10 | | | |

a. For each variable, coefficient estimates are shown with the following significance codes: 0 '***'; 0.001 '**'; 0.01 '*'; 0.05 '.'.

b. Model is a weighted linear regression model of adjusted eGFR slope (weight = inverse variance of adjusted eGFR slope). Base model includes variables: baseline eGFR, Diabetes, and Age. Models A and B include base variables with the addition of methylation level at probe location, methylation batch, and bisulfite conversion efficiency.

c. Proportion of variance explained by the variable based on conditional sum of squares calculated in Type II ANOVA analysis.

Supplementary Table 9. Gene Ontology for top methylation probes that improve model of kidney function

| Category | Term | RT | Genes | Count | % | P-Value | Benjamini |
|-------------|---|----|-------|-------|------|----------|-----------|
| GOTERM_BP_1 | developmental process | RT | | 131 | 40.6 | 3.70E-05 | 8.50E-04 |
| GOTERM_BP_1 | biological adhesion | RT | | 47 | 14.6 | 1.50E-03 | 1.70E-02 |
| GOTERM_BP_1 | signaling | RT | | 134 | 41.5 | 1.60E-03 | 1.20E-02 |
| GOTERM_BP_1 | response to stimulus | RT | | 169 | 52.3 | 2.50E-03 | 1.40E-02 |
| GOTERM_BP_1 | single-organism process | RT | | 250 | 77.4 | 3.80E-03 | 1.80E-02 |
| GOTERM_BP_1 | localization | RT | | 124 | 38.4 | 4.80E-03 | 1.80E-02 |
| GOTERM_BP_1 | regulation of biological process | RT | | 209 | 64.7 | 8.70E-03 | 2.80E-02 |
| GOTERM_BP_1 | biological regulation | RT | | 219 | 67.8 | 9.50E-03 | 2.70E-02 |
| GOTERM_BP_1 | multicellular organismal process | RT | | 142 | 44 | 1.10E-02 | 2.80E-02 |
| GOTERM_BP_1 | cellular component organization or biogenesis | RT | | 125 | 38.7 | 3.10E-02 | 7.00E-02 |
| GOTERM_BP_1 | growth | RT | | 25 | 7.7 | 3.40E-02 | 6.90E-02 |
| GOTERM_BP_1 | immune system process | RT | | 54 | 16.7 | 5.10E-02 | 9.60E-02 |
| GOTERM_BP_1 | locomotion | RT | | 35 | 10.8 | 7.60E-02 | 1.30E-01 |
| GOTERM_BP_1 | cellular process | RT | | 276 | 85.4 | 8.90E-02 | 1.40E-01 |

!